



HAL
open science

Paracatadioptric visual servoing from lines

H Hadj Abdelkader, Y. Mezouar, Philippe Martinet

► **To cite this version:**

H Hadj Abdelkader, Y. Mezouar, Philippe Martinet. Paracatadioptric visual servoing from lines. 35th International Symposium on Robotics, ISR'04, Mar 2004, Paris, France. hal-02467050

HAL Id: hal-02467050

<https://inria.hal.science/hal-02467050>

Submitted on 4 Feb 2020

HAL is a multi-disciplinary open access archive for the deposit and dissemination of scientific research documents, whether they are published or not. The documents may come from teaching and research institutions in France or abroad, or from public or private research centers.

L'archive ouverte pluridisciplinaire **HAL**, est destinée au dépôt et à la diffusion de documents scientifiques de niveau recherche, publiés ou non, émanant des établissements d'enseignement et de recherche français ou étrangers, des laboratoires publics ou privés.

Paracatadioptric visual servoing from lines

H. Hadj Abdelkader

Y. Mezouar

P. Martinet

LASMEA

24 avenue des Landais
63177 AUBIERE - FRANCE
hadj,mezouar,martinet@lasmea.univ-bpclermont.fr

Abstract

In this paper we present a new approach to control the 6 degrees of freedom of a manipulator using the projection of 3D lines extracted from the image plane of an omnidirectional camera. The main motivation of this work is to overcome the problem of visibility when using classical vision sensor. Indeed one of the principal deficiency of classical visual servoing strategy is that some parts of the visual features may get out of the field of view during servoing leading to its failure. Panoramic cameras overcome this problem because of their wider field of view. The present paper is concerned with the use of lines in paracatadioptric visual servoing. Indeed when dealing with real environments (indoor or outdoor) or industrial workpiece, the extraction and the tracking of lines is natural. We derive the panoramic image jacobian for lines in the case of image based visual servoing. The corresponding control law is then designed and validated.

Keywords

Visual Servoing, Omnidirectional camera, lines

1 Introduction

In the last years, the use of visual observations to control the motions of robots has been extensively studied (approach referred in the literature as visual servoing). The advent of fast and inexpensive digital imaging technology has allowed camera systems to be integrated as part of a closed loop feedback control system. Computer vision can provide to the robotic system a powerful way of sensing the environment and can potentially reduce or obliterate the need for environmental modeling, which is extremely important when the robotic tasks require the robot to move in unknown and/or dynamic environments.

Conventional cameras suffer from restricted field of view. Many applications in vision-based robotics, such as mobile

robot localisation [5] and navigation [23], can benefit from panoramic field of view provided by omnidirectional cameras. In the literature, there have been several methods proposed for increasing the field of view of cameras systems. One effective way is to combine mirrors with conventional imaging system. The obtained sensors are referred as catadioptric imaging systems. The resulting imaging systems have been termed central catadioptric when a single projection center describe the world-image mapping. From a practical view point, a single center of projection is a desirable property for an imaging system [2]. Baker and Nayar in [2] derive the entire class of catadioptric systems with a single viewpoint.

The visual servoing framework is an effective way to control robot motions from cameras observations [12]. Control of motion with omnidirectional cameras appears in the literature for mobile robot formation control [20], [22]. Visual servoing schemes are generally classified in three groups, namely position-based, image-based and hybrid-based control [11, 12, 15]. Classical visual servoing techniques make assumptions on the link between the initial, current and desired images. They require correspondences between the visual features extracted from the initial image with those obtained from the desired one. These features are then tracked during the camera (and/or the object) motion. If these steps fail the visually based robotic task can not be achieved [6]. Typical cases of failure arise when matching joint images features is impossible (for example when no joint features belongs to initial and desired images) or when some parts of the visual features get out of the field of view during the servoing. Some methods has been proposed to resolve this deficiency based on path planning [18], switching control [7], zoom adjustment [13], geometrical and topological considerations [10]. However, such strategies are sometimes delicate to adapt to generic setup.

Clearly, visual servoing applications can also benefit from cameras with a wide field of view. The image Jacobian

(also termed interaction matrix) play a central role to design vision-based control law. It links the variations of image observations to the camera velocity. The analytical form of the interaction matrix is available for some image features (points, circles, lines, \dots) in the case of conventional cameras [11]. As explained, omnidirectional view can be a powerful way to overcome the problem of target visibility in visual servoing. Barreto *et al.* in [3], studied the central catadioptric Jacobian matrix for a set of image points. This paper is mainly concerned with the use of projected lines extracted from central catadioptric images as input of a visual servoing. When dealing with real environments (indoor or outdoor) or industrial workpiece, lines features are natural choices. Nevertheless, most of the effort in visual servoing are devoted to points [12], only few works have investigated the use of lines in visual servoing with traditional cameras (refer for example to [1], [14]) and none has explored the case of omnidirectional cameras. This paper is concerned with this last issue, we derive a form of the central paracatadioptric image Jacobian for lines which can be exploited to design a control law for positioning task of a six degrees of freedom manipulator.

The remainder of this paper is organized as follow. In Section 2, following the description of the central catadioptric camera model, lines projections in the image plane is studied. This is achieved using the paracatadioptric camera. We present, in Section 3 the control law and we derive a form of the image Jacobian for paracatadioptric projected lines. In Section 4, simulated results are presented.

2 Central paracatadioptric image formation of lines

In this section, we describe the projection model for central paracatadioptric cameras and then we focus on 3D lines features.

2.1 Paracatadioptric camera model

As noted previously, a single center of projection is a desirable property for an imaging system. A single center implies that all lines passing through a 3D point and its projection in the image plane pass through a single point in 3D space. Conventional perspective cameras are single view point sensors. As shown in [2], a central catadioptric system can be build by combining an hyperbolic, elliptical or planar mirror with a perspective camera and a parabolic mirror with an orthographic camera.

In this paper, we will thus study only the last configuration (parabolic mirror with an orthographic camera). The camera model expresses the bond between space 3D and space 2D (*image*). The orthographic camera model is gi-

ven by :

$$\begin{pmatrix} \mathbf{p} \\ 1 \end{pmatrix} = \alpha \begin{pmatrix} 1 & 0 & 0 & 0 \\ 0 & 1 & 0 & 0 \\ 0 & 0 & 0 & 1 \end{pmatrix} \begin{pmatrix} \mathbf{R} & \mathbf{t} \\ 0_{3 \times 3} & 1 \end{pmatrix} \begin{pmatrix} \mathbf{P}_w \\ 1 \end{pmatrix} \quad (1)$$

$$\underline{\mathbf{u}} = \mathbf{K}\mathbf{p}$$

where $\mathbf{P}_w = [X \ Y \ Z]^T$ is the coordinates of point \mathcal{P} with respect to \mathcal{F}_w (world frame), \mathbf{R} and \mathbf{t} are rotation matrix and translation vector respectively between \mathcal{R}_w and \mathcal{F}_c (camera frame). \mathbf{K} denote the triangular calibration matrix, $\mathbf{p} = [x \ y \ 1]^T$ the metric homogenous coordinates of image point, $\underline{\mathbf{u}} = [u \ v \ 1]^T$ is $\underline{\mathbf{p}}$ expressed on pixel, α is a non-zero scale factor.

According to the projection model [3], \mathbf{P}_w is projected in the image plan of paracatadioptric sensor to a point $\underline{\mathbf{u}}$ with:

$$\underline{\mathbf{u}} = \mathbf{K}\mathbf{M}\mathbf{f}(\mathbf{X}) \quad (2)$$

where :

$$\mathbf{M} = \begin{bmatrix} 2p & 0 & 0 \\ 0 & 2p & 0 \\ 0 & 0 & 1 \end{bmatrix}$$

and :

$$\mathbf{f}(\mathbf{X}) = \begin{pmatrix} \frac{X}{Z + \sqrt{X^2 + Y^2 + Z^2}} \\ \frac{Y}{Z + \sqrt{X^2 + Y^2 + Z^2}} \\ 1 \end{pmatrix} \quad (3)$$

In the sequel, we will assume without loss of generality that the \mathbf{K} -matrix is the identity, the mapping function describing central catadioptric projection is then given by:

$$\underline{\mathbf{u}} = \mathbf{M}\mathbf{f}(\mathbf{X}) \quad (4)$$

2.2 Projection of Lines

In order to model lines projections in the image of a central paracatadioptric imaging system, we use the Plücker coordinates of lines. Let (\mathfrak{S}) be a 3D line, these Plücker's coordinate are defined as :

$$(\mathfrak{S}) : \begin{pmatrix} \mathbf{n} \\ \mathbf{u} \end{pmatrix} \quad (5)$$

where \mathbf{u} is a unit vector lies in the line (\mathfrak{S}) , and \mathbf{n} defined by:

$$\mathbf{n} = \mathbf{P} \times \mathbf{u} \quad (6)$$

where \mathbf{P} is a point in (\mathfrak{S}) .

The interpretation plan contain the line in space and the central point of the paracatadioptric system, and its equation is given by :

$$(\Pi) : n_x x + n_y y + n_z z = 0 \quad (7)$$

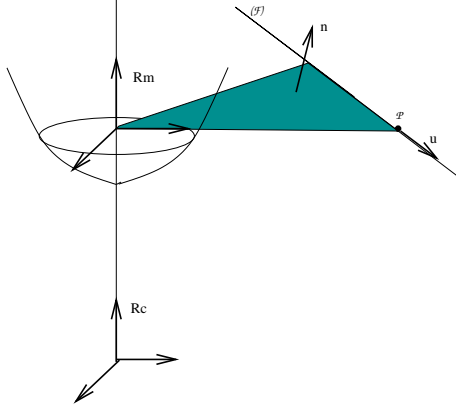


FIG. 1 – Paracatadioptric line images

The orthographical camera is placed so that the projection of the rays coming from the surface of the parabolic mirror is orthographical on CCD plan of the camera. For this purpose, axis Z of the camera is confused with the axis of symmetry Z of the mirror (see Figure 1).

The equation of the corresponding parabolic mirror is given by :

$$z = \frac{x^2 + y^2}{2a_p} - \frac{a_p}{2} \quad (8)$$

$$a_p = 2p$$

where p is the parameter of the parabola. Let (S_p) be the intersection between the interpretation plan (Π) and the surface mirror. (S_p) defines the line projection in the mirror surface. The points $\mathbf{p} = [x \ y \ z]^T$ in \mathcal{F}_m from the set (S_p) verify two constraints. On one hand, the points \mathbf{p} must lie in the surface mirror, so verify the equation (8). On the other hand, they lie in the plan (Π) , so satisfy the equation (7). By combining between (7) and (8), we proof that :

$$\underline{\mathbf{p}}^T \mathbf{A}_p \underline{\mathbf{p}} = 0 \quad (9)$$

where $\underline{\mathbf{p}} = [x \ y \ 1]^T$ and

$$\mathbf{A}_p = \begin{pmatrix} n_z & 0 & a_p n_x \\ 0 & n_z & a_p n_y \\ a_p n_x & a_p n_y & -a_p^2 n_z \end{pmatrix} \quad (10)$$

The quadratic equation given in (10) is a circle, depend the both mirror parameters and the interpretation plan (Π) . Let \mathbf{R}_c the rotation matrix between the camera frame and world frame. Without loss of generality, we are going to assume $\mathbf{R}_c = \mathbf{I}$.

Using the intrinsic parameters matrix, the equation (9) can be written in the pixel dimension as :

$$\underline{\mathbf{u}}^T \mathbf{K}^{-T} \mathbf{A}_p \mathbf{K}^{-1} \underline{\mathbf{u}} = 0 \quad (11)$$

The paracatadioptric image of line in pixel dimension is a always circle/ellipse (equation (11)).

Later on, and without loss the generality, we assume $\mathbf{K} = \mathbf{I}_{3 \times 3}$. So the quadratic equation given by (10) defines the mapping lines in the paracatadioptric image plan.

$$\begin{cases} A_{p0} = n_z \\ A_{p1} = n_z \\ A_{p2} = 0 \\ A_{p3} = a_p n_x \\ A_{p4} = a_p n_y \\ A_{p5} = -a_p^2 n_z \end{cases} \quad (12)$$

3 Control law

In order to control the movements of a robot from visual information, we define a task function as [21] :

$$\mathbf{e} = \hat{\mathbf{L}}^+ (\mathbf{s} - \mathbf{s}^*) \quad (13)$$

where :

- \mathbf{s} is composed of the current features extracted from the catadioptric image. We will define this vector in the following.
- \mathbf{s}^* is the desired value of \mathbf{s}
- \mathbf{L}^+ is the pseudo-inverse of model of the interaction matrix \mathbf{L} . The interaction matrix \mathbf{L} is the jacobian defined as :

$$\mathbf{L} = \frac{\partial \mathbf{s}}{\partial \mathbf{r}} \quad (14)$$

It binds the variations of the visual features to the screw Vector camera $\mathbf{T} = \dot{\mathbf{r}} = [\mathbf{V}, \mathbf{W}]^T$:

$$\dot{\mathbf{s}} = \mathbf{L} \mathbf{T} \quad (15)$$

If we wishes an exponential decreasing of the task function \mathbf{e} towards $\mathbf{0}$ and if the scene is supposed to be static, the law control is given by :

$$\mathbf{T} = -\lambda \hat{\mathbf{L}}^+ (\mathbf{s} - \mathbf{s}^*) \quad (16)$$

The jacobian matrix \mathbf{L} thus plays a central role for the synthesis of control law. In the continuation, after having chosen the vector of visual features \mathbf{s} , we give the analytical forme of the interaction matrix for the combinations parabolic mirror-orthographical camera.

The coefficients A_{pi} of the quadratic forme (to refer to (12)) are defined except for a non-zero factor constant. In order to use these coefficients in the control loop, it is thus necessary to eliminate this factor. We can for that divide each coefficient of the quadratic form by a linear combination adequate of those. In order to minimize the whole of the degenerated configurations (such as the parameter of standardization is null), we chose A_{h5} like parameter of standardization where this situation is presented on the

$n_z = 0$ (i.e. the interpretation plan contain de Z axis of the mirror frame). In this case, the whole of the degenerated configurations for the interpretation plan is the plan $n_z = 0$. The vector of the visual features is thus:

$$\mathbf{s} = \begin{pmatrix} \frac{A_{p3}}{A_{p5}} \\ \frac{A_{p4}}{A_{p5}} \end{pmatrix} \quad (17)$$

The calculation of the interaction matrix appropriate to this vector of features is based on the following decomposition :

$$\mathbf{L} = \frac{\partial \mathbf{s}}{\partial \mathbf{r}} = \frac{\partial \mathbf{s}}{\partial \mathbf{n}} \frac{\partial \mathbf{n}}{\partial \mathbf{r}} \quad (18)$$

The first term $\frac{\partial \mathbf{s}}{\partial \mathbf{n}}$ represent the interaction between the visual features motion in the image and the normal vector motion. The second term $\frac{\partial \mathbf{n}}{\partial \mathbf{r}}$ bind the normal vector motion to the camera motion. By noting that :

$$\begin{cases} \dot{\mathbf{u}} = -\mathbf{W} \times \mathbf{u} \\ \dot{\mathbf{n}} = -\mathbf{V} \times \mathbf{u} - \mathbf{W} \times \mathbf{n} \end{cases} \quad (19)$$

We obtain the interaction between the variations of the normal vector and the movements of the camera :

$$\frac{\partial \mathbf{n}}{\partial \mathbf{r}} = \begin{pmatrix} 0 & -u_z & u_y & 0 & -n_z & n_y \\ u_z & 0 & -u_x & n_z & 0 & -n_x \\ -u_y & u_x & 0 & -n_y & n_x & 0 \end{pmatrix} \quad (20)$$

The interaction between the movement of the visual features in the image and the variations of the normal vector to the plan of interpretation is easily obtained by deriving (??) to the components of \mathbf{n} :

$$\frac{\partial \mathbf{s}}{\partial \mathbf{n}} = \frac{1}{a_p n_z} \begin{pmatrix} -1 & 0 & \frac{n_x}{n_z} \\ 0 & -1 & \frac{n_y}{n_z} \end{pmatrix} \quad (21)$$

The interaction matrix is then obtained by (18), and it can be written $\mathbf{L} = [\mathbf{A} \ \mathbf{B}]$ with:

$$\mathbf{A} = -\frac{1}{a_p n_z} \begin{pmatrix} -\frac{n_x u_y}{n_z} & u_z + \frac{n_x u_x}{n_z} & -u_y \\ -u_z - \frac{n_y u_y}{n_z} & \frac{n_y u_x}{n_z} & u_x \end{pmatrix}$$

and

$$\mathbf{B} = -\frac{1}{a_p n_z} \begin{pmatrix} -\frac{n_x n_y}{n_z} & 1 + \frac{n_x^2}{n_z} & -n_y \\ -1 - \frac{n_y^2}{n_z} & \frac{n_x n_y}{n_z} & n_x \end{pmatrix}$$

This jacobian has a rank 2, its kernel is given by the following vectors :

$$\begin{cases} (1, -\frac{u_3 n_z^2 + u_3 n_x^2 + n_y n_z u_2}{n_y (u_3 n_x - u_1 n_z)}, 0, 0, \frac{u_3 n_x u_1 + u_3 n_y u_2 + u_3^2 n_z}{n_y (u_3 n_x - u_1 n_z)}, 0) \\ (0, \frac{n_x^3 + n_x n_y^2 + n_x n_z^2}{n_y (u_3 n_x - u_1 n_z)}, 0, 0, -\frac{u_3 n_x n_z + n_y^2 u_1 + n_x^2 u_1}{n_y (u_3 n_x - u_1 n_z)}, 1) \\ (0, \frac{n_x n_y u_2 + n_x^2 u_1 + u_1 n_z^2}{n_y (u_3 n_x - u_1 n_z)}, 1, 0, -\frac{n_z u_3 u_1 + n_y u_1 u_2 + n_x u_1^2}{n_y (u_3 n_x - u_1 n_z)}, 0) \\ (0, -\frac{n_z^3 + n_y n_z^2 + n_z n_x^2}{n_y (u_3 n_x - u_1 n_z)}, 0, 1, \frac{u_3 n_z^2 + n_x u_1 n_z + u_3 n_y^2}{n_y (u_3 n_x - u_1 n_z)}, 0) \end{cases}$$

One thus needs at least three lines to control the six degrees of freedom of the camera. If one considers a set of N lines, the corresponding matrix of interaction is :

$$\mathbf{L} = [\mathbf{L}_1^T \ \dots \ \mathbf{L}_n^T]^T$$

4 Results

In this part, we present simulation results of paracatadioptric visual servoing from lines by using the control law (25). In the results of simulation which we will present, the initial attitude of the reference camera in comparison to the world reference is given by $\mathbf{r}_i = [0, 0, 1, 0, 0, 0]^T$ (the first three terms of \mathbf{r}_i are the components of translation in meter and last three are the components of rotation in radian). The desired image is acquired at the position of the camera given by $\mathbf{r}_d = [0.1, 0.1, 1.1, \frac{\pi}{8}, \frac{\pi}{8}, \frac{\pi}{8}]^T$. The three lines used during visual servoing are defined in the world space by the following plucker-coordinates :

$$\begin{cases} (\mathfrak{S}1) : \begin{pmatrix} u_1 = (0 \ 1 \ 0)^T \\ n_1 = (0 \ 0 \ -1)^T \end{pmatrix} \\ (\mathfrak{S}2) : \begin{pmatrix} u_2 = (0 \ 0.9806 \ 0.1961)^T \\ n_2 = (0 \ -0.1961 \ 0.9806)^T \end{pmatrix} \\ (\mathfrak{S}3) : \begin{pmatrix} u_3 = (0.9623 \ 0.1925 \ 0.1925)^T \\ n_3 = (0.1961 \ 0 \ -0.9806)^T \end{pmatrix} \end{cases}$$

Figure 2 show the initial spacial configuration of lines and camera. Image noise has been introduced (additive noise whit maximum amplitude of 1 pixel). The images corresponding to the initial and desired cameras positions are given in figures 3(a) and 3(b). Figure 3(c) shows the trajectory of the conics in the image plan. Camera velocities are given in figure 4. As one can note it on the figures 5 of errors between desired and current feature vectors, the task of positioning is correctly carried out.

5 Conclusion

In this paper, we have present a strategy of the control manipulators robots at six degrees of freedom using a paracatadioptric visual features from lines in the control loop. The interaction matrix was obtained in the cases of the combinations parabolic mirror-orthographical camera, what allowed to construct an adequate control law. In the continuation of this work we wish studied the case of the nonholonomic mobile robots.

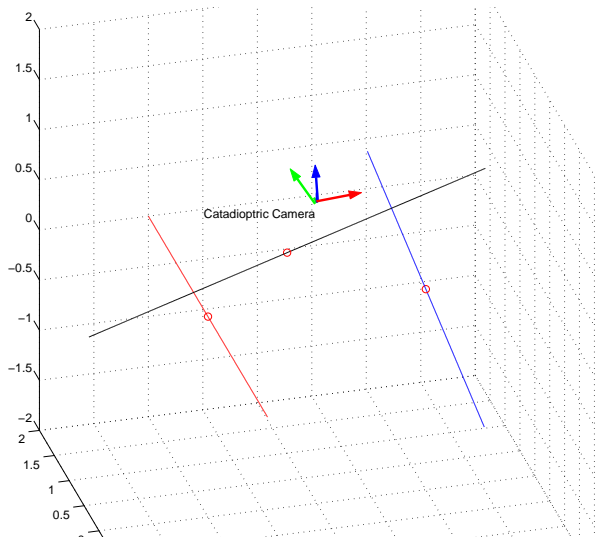


FIG. 2 – 3D scene

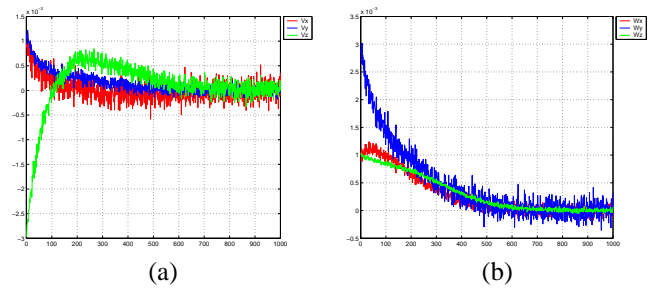


FIG. 4 – (a) Translational velocities [m/s] and (b) rotational velocities [rad/s]

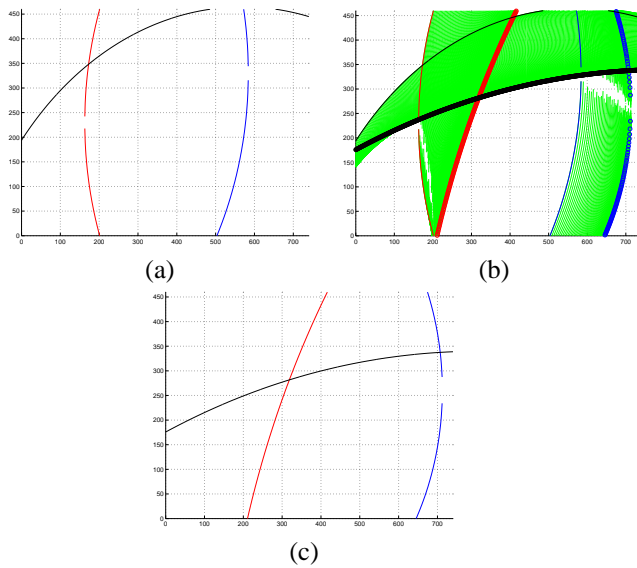


FIG. 3 – (a) Initial image, (b) trajectory of the catadioptric image lines, (c) desired image

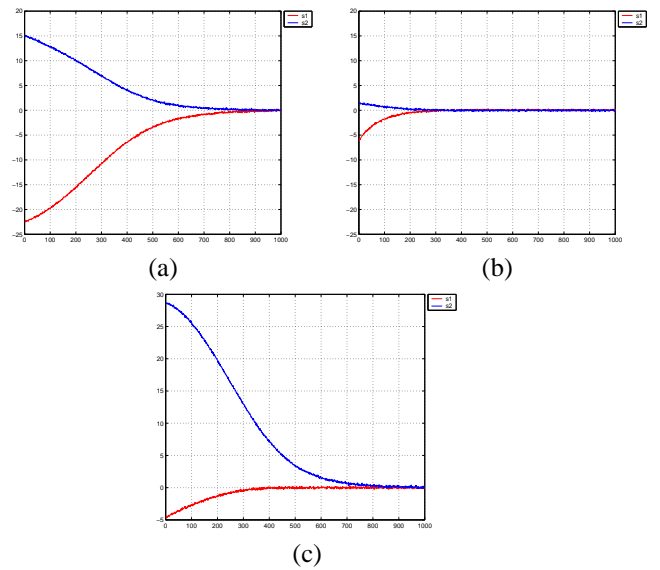


FIG. 5 – (a) Errors for the first conic, (b) Errors for the second conic, (c) Errors for the third conic

Références

- [1] N. Andreff, B. Espiau, and R. Horaud. Visual servoing from lines. *International Journal of Robotics Research*, 21(8), August 2002.
- [2] S. Baker and S. K. Nayar. A theory of single-viewpoint catadioptric image formation. *International Journal of Computer Vision*, 35(2):1–22, November 1999.
- [3] J. P. Barreto, F. Martin and R. Horaud. Visual servoing/tracking using central catadioptric images. Dans *ISER2002 - 8th International Symposium on Experimental Robotics*, Juillet 2002.
- [4] R. Benosman and S. Kang. *Panoramic Vision*. Springer Verlag, 2000.
- [5] P. Blaer and P.K. Allen. Topological mobile robot localization using fast vision techniques. In *IEEE Int. Conference on Robotics and Automation*, pages 1031–1036, Washington, May 2002.
- [6] F. Chaumette. Potential problems of stability and convergence in image-based and position-based visual servoing. *The Confluence of Vision and Control*, D. Kriegman, G. Hager, A. Morse (eds), *LNCIS Series*, Springer Verlag, 237:66–78, 1998.
- [7] G. Chesi, K. Hashimoto, D. Prattichizzo, and A. Vicino. A switching control law for keeping features in the field of view in eye-in-hand visual servoing. In *IEEE Int. Conf. on Robotics and Automation*, pages 3929–3934, Taipei, Taiwan, 2003.
- [8] P. Corke and S. Hutchinson. A new partitioned approach to image-based visual servo control. Dans *IEEE Conference on Decision and Control*, pages 2521–2526, Sydney, Décembre 2000.
- [9] N.J. Cowan, G.A.D. Lopes, and D.E. Koditschek. Rigid body visual servoing using navigation functions. Dans *IEEE Int. Conf. on Decision and Control*, pages 3920–3926, Sydney, Australie, 2000.
- [10] Noah J. Cowan, Joel D. Weingarten, and Daniel E. Koditschek. Visual servoing via navigation functions. *Transactions on Robotics and Automation*, August 2002.
- [11] B. Espiau, F. Chaumette, and P. Rives. A new approach to visual servoing in robotics. *IEEE Trans. on Robotics and Automation*, 8(3):313–326, June 1992.
- [12] S. Hutchinson, G.D. Hager, and P.I. Corke. A tutorial on visual servo control. *IEEE Trans. on Robotics and Automation*, 12(5):651–670, October 1996.
- [13] E. Malis S. Benhimane. Vision-based control with respect to planar and non-planar objects using a zooming camera. Dans *IEEE International Conference on Advanced Robotics*, Juillet 2003.
- [14] E. Malis, J. Borrelly, and P. Rives. Intrinsic-free visual servoing with respect to straight lines. In *IEEE/RSJ International Conference on Intelligent Robots Systems*, Lausanne, Switzerland, October 2002.
- [15] E. Malis, F. Chaumette, and S. Boudet. 2 1/2 d visual servoing. *IEEE Trans. on Robotics and Automation*, 15(2):238–250, April 1999.
- [16] E. Malis, F. Chaumette, and S. Boudet. Positioning a coarse-calibrated camera with respect to an unknown object by 2d 1/2 visual servoing. *IEEE Int. Conference on Robotics and Automation*, 2:1352–1359, Mai 1998.
- [17] P. Martinet and J. Gallice. Position based visual servoing using a nonlinear approach. Dans *IEEE/RSJ International Conference on Intelligent Robots and Systems*, volume 1, pages 531–536, Kyongju, Corée du Sud, Octobre 1999.
- [18] Y. Mezouar and F. Chaumette. Path planning for robust image-based control. *IEEE Trans. on Robotics and Automation*, 18(4):534–549, August 2002.
- [19] T. Pajdla, T. Svoboda, and V. Hlavac. *Panoramic Vision : Sensors, Theory and Applications*, chapter Epipolar Geometry of Central Panoramic Catadioptric Cameras, pages 73–102. R. Benosman and S. B. Kang, 2001.
- [20] A. Paulino and H. Araujo. Multiple robots in geometric formation: Control structure. In *Int. Symposium on Intelligent Robotic Systems*, UK, 2000.
- [21] C. Samson and B. Espiau. Application of the task function approach to sensor-based-control of robot manipulators. In *11th IFAC World Congress*, volume 9, pages 286–291, Tallin, Estonie, URSS, Aout 1990.
- [22] R. Vidal, O. Shakernia, and S. Sastry. Formation control of nonholonomic mobile robots with omnidirectional visual servoing and motion segmentation. In *IEEE International Conference on Robotics and Automation*, Taipei, Taiwan, 2003.
- [23] N. Winter, J. Gaspar, G. Lacey, and J. Santos-Victor. Omnidirectional vision for robot navigation. In *OMNIVIS*, pages 21–28, 2000.